Considerations on the presence of gravity wave activity during MCS limb staring observations

R. M. Edmonds , *Department of Astronomy, New Mexico State University, Las Cruces, New Mexico, USA (redmonds@nmsu.edu),* **J. Murphy**, *Department of Astronomy, New Mexico State University, Las Cruces, New Mexico, USA*, **J. T. Schofield**, *Jet Propulsion Laboratory, California Institute of Technology, Pasadena, California, USA.*, **N. G. Heavens**, *Hampton University, Hampton, VA, USA.*

Introduction:

Heavens et al. [2010] (hereafter *H2010*) identified an enhanced frequency, with respect to MY29, of convective instabilities at northern latitudes and low (~0.1 Pa) pressures in MY28 Mars Climate Sounder (MCS) observations of the Martian atmosphere for several months before the MY28 global dust storm. The pre-MY 28 global dust storm convective instabilities were thought to be the result of gravity wave breaking, and were contemporaneous with 0.1 Pa temperatures at northern equatorial regions being abnormally cool. As a result of these observations a causative link between gravity waves, equatorial temperatures, and global dust storm development was suggested by *H2010*.

MY28 MCS observations before the MY28 global dust storm were conducted in an abnormal 'limb staring' mode. During this time, calibration views of space and calibration targets were not conducted. This resulted in zero signal offset variation in radiance measurements during this time. We have identified variability in convective instabilities and cool equatorial temperatures being highly coincident with a change in observing mode, suggesting the observed cooling and variability of convective instabilities during limb staring are an artifact of the observing mode.

We conducted a simple approximate analysis to determine whether offset variation can affect observations of convective instabilities during MY28. Our analysis suggests that a significant fraction of instabilities detected by *H2010* may not contain a real instability. However, our analysis is inconclusive in ruling out all variability.

We have also explored through modeling whether gravity breaking, resulting in drag on the mean flow, can account for the observed cooling. The modeling was conducted using the NASA Ames Research Center Mars General Circulation Model (ARC-MGCM), and applying additional drag to the zonal flow to simulate the effect of gravity wave breaking. Through the modeling we cannot reproduce the magnitude of the cooling observed at 0.1 Pa and equatorial latitudes by MCS during MY28, supporting the idea the variability is an artifact of the observing mode.

MCS Data:

MCS is an instrument aboard Mars Reconnaissance Orbiter (MRO). The instrument collects limb, nadir, and off nadir radiance measurements of the Martian atmosphere for nine different spectral channels [*McCleese et al.*, 2007]. For each channel there are 21 detectors that are spaced to record the vertical structure of the IR emission. Vertical temperature profiles have been derived through modeling the radiance measurements as described by *Kleinböhl et al.* [2009]. The temperature data typically extends from the surface to ~80 km with ~5 km resolution. Temperatures from ~40-80 km are derived using the MCS "A3" channel which is centered at 15.4 μm.

In normal operation MCS conducts calibration observations of space using all 21 detectors. The observations of space provide information for determining zero signal offset corrections. MCS from February 9th, 2007 (L_s 180.7°) to June 14th, 2007 (L_s 257.1°) operated abnormally in a "limb staring" mode. During this abnormal operation calibration views were not conducted, and the instruments view of the limb drifted through orbit. Due to the view of the limb drifting vertically through an orbit, offset variation can be occasionally assessed through an orbit. This assessment of offset variation was not used in calibrating the radiance measurements, but we note that offset varied ~0.15 milliWatts/m^2/sr/cm^{-1} over a timeframe of hours to days.

The MCS derived temperatures used in our analysis makes use of a new version, version 4, not available to *H2010*. Version 4 applies small geometry corrections, and a climatological pressure retrieval scheme. The new versions generally provide more retrieved profiles, and better derivation of the retrieved temperatures. The temperature data available to our analysis also extends almost an additional two MYs.

Analysis:

Interested in exploring the possibility of gravity waves playing a role in global dust storm development, we initially intended to reproduce *H2010*'s analysis of convective instabilities and expand upon the work. Convective instabilities in *H2010* analysis were identified by determining whether a profile contained maximum Convective Atmospheric Potential Energy ($CAPE_{MA}$) above a threshold of 300 J kg^{-1}. This threshold was determined from error analysis, which did not account for offset variation, provided a 95% confidence that the profile at least contained an instability (i.e. the true $CAPE_{MA}$ for the

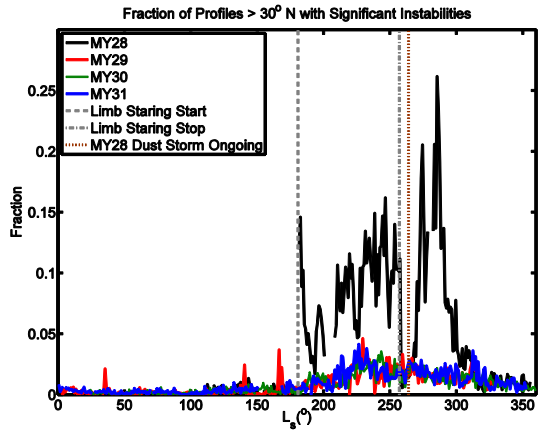

Figure 1: The fraction of profiles containing significant instabilities for latitudes > 30° N binned at 1° of Ls. Vertical dashed lines correspond to events only in MY 28. The latitude range presented in the figure is where the majority of significant instabilities were reported by *Heavens et al.* [2010].

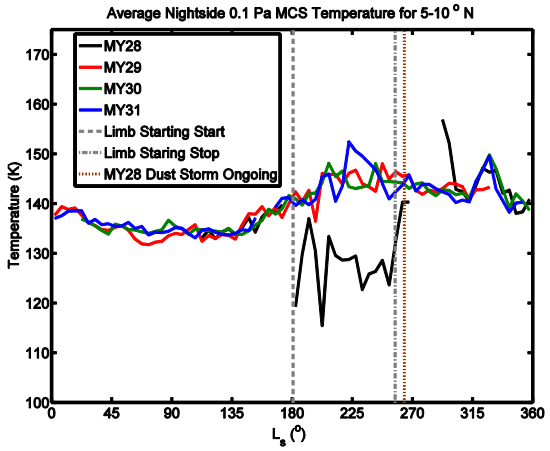

Figure 2: Average 0.1 Pa MCS night-side temperatures between 5-10° N binned at 5° of L_s. Vertical dashed lines correspond to events only in MY 28.

profile was > 0 J kg^{-1}). The profiles which met this threshold were said to contain a "significant instability".

We identified the enhanced frequency of significant instabilities in MY28 MCS data before and during the MY28 global dust storm. We also identified a brief drop in the frequency for ~10° L_s before the frequency of the instabilities again increased during the MY28 global dust storm. This drop in the frequency closely coincided with a change in observing mode (Fig. 1).

MY28 MCS temperatures during 'limb staring` at northern equatorial latitudes were found to be ~25-15K cooler relative to all other MYs observed by MCS. However, the MCS temperatures warmed when the instrument stopped limb staring operation and returned to normal operation (Fig. 2). This warming was not found by *H2010* to coincide with the change in observing mode in earlier versions of the MCS data. The variation in MCS temperatures and significant instabilities with a change in observing mode on its own is highly suggestive of the enhanced frequency of significant instabilities and equatorial cool temperatures during limb staring being an artifact of the limb staring observing mode. The increased frequency of the significant instabilities *during* the MY28 dust storm may be real, since the MCS instrument had returned to normal operation by the time the MY 28 global dust storm had begun.

We conducted analysis to explore whether zero signal offset variation can produce a non-negligible effect on the occurrence of significant instabilities and temperatures during limb staring. Because re-deriving MCS temperatures via using *Kleinböhl et al.*'s [2009] methodology is computationally and man-hour expensive, we explored the effect of offset through an approximate method.

We assumed the measured radiance in the "A3" channel, L_m is determined by,

$$L_m(z) = \varepsilon_m(z) B_{\tilde{\nu}}\big(T(z)\big) + L_0, \qquad (1)$$

where ε is the emissivity, B_ν is the Plank function in terms of wavenumber, T is the MCS derived temperature, z is the altitude, and L_0 is the zero signal offset correction. The Planck function is a function of temperature. Temperature, emissivity, and measured radiance are considered functions of altitude. For our approximate analysis it is sufficient to consider the Planck function at the "A3" channel's center in wavelength.

Radiance measurements are recorded as functions of detector. To consider radiance as function of altitude, the measurements were interpolated to altitude assuming the radiance was emitted directly over the scene. MCS derived temperatures are averaged from 5 radiance measurements. For our approximate analysis we consider only the time centered radiance profile from which a temperature profile was derived, which is sufficient for our approximate analysis.

Since emissivity is not a standard derived output from *Kleinböhl et al.*'s [2009] modeling, we determine emissivity values as a function of altitude. This is conducted by solving for emissivity in Eq. 1. We then calculate emissivity values by applying our radiance measurements interpolated to altitude, MCS temperatures values, and assume no offset correction. With our derived emissivity values and MCS radiance measurements interpolated to altitude we can then solve for new temperatures using Eq. 1 considering different offset corrections.

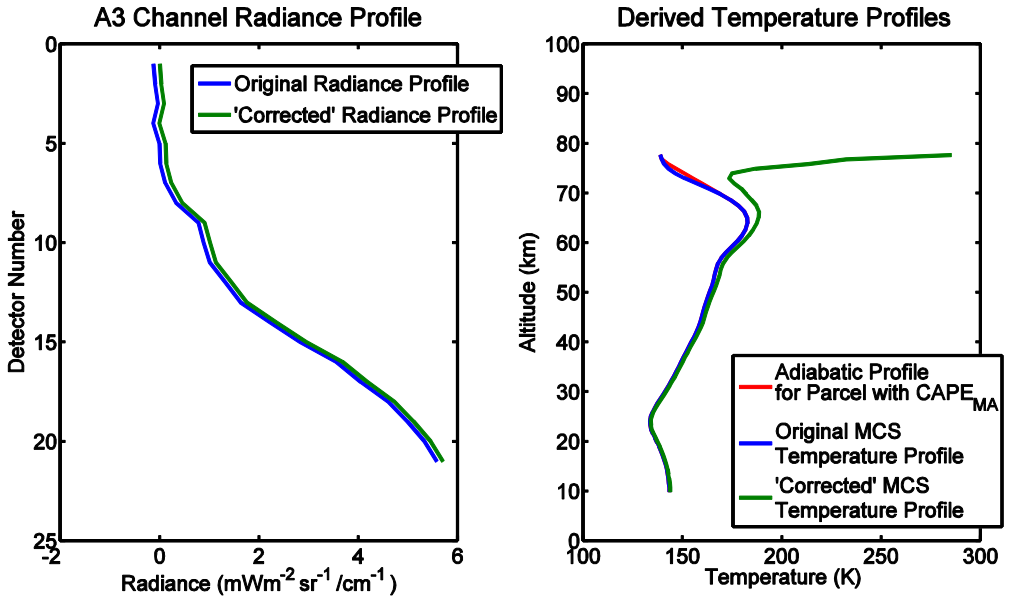

Figure 3: In the right most plot is an MCS temperature profile (blue) containing a significant instability from May 12th, 2007 (L_s 236°) 54° N 143° W and the offset corrected temperature profile (green) using our approximate method which no longer containing a significant instability. The offset correction of 0.1003 milli-Watts/m^2/sr/cm^{-1} was added to all detectors to make the top most detector radiance equal to zero. The red temperature profile is the adiabatic temperature of the parcel with $CAPE_{MA}$ assuming adiabatic cooling while being lifted vertically. This corrected profile contained no CAPE > 0 J kg^{-1}. The offset corrected temperature profile contained no $CAPE_{MA}$ > 0 J kg^{-1}. Plotted to the left is the radiance and offset corrected MCS radiance profile used in deriving the temperature profiles to the right.

We re-derived temperatures for profiles containing significant instabilities via our approximate method. We explored the effect of considering the top looking "A3" channel detector radiance as being representative of an appropriate offset correction (e.g. Fig. 3). This measurement, typically not used for these profiles in the derivation of the MCS temperature profiles, does provide some information about offset. This is because at northern latitudes the MCS instrument view for the top most looking detectors drifts toward space looking views.

Using the top looking detector "A3" radiance measurements to determine zero signal offset corrections, we found 42% of profiles that contained a significant instability no longer contained a significant instability. We also interpolated between times where there were no top looking detectors with space views, but were unable to further remove instabilities from MCS profiles. However, our analysis should at least highlight that offset variation can impose a not insignificant effect on the profile containing an instability. While we cannot conclude offset variation can account for all of the enhanced frequency of MCS profiles containing a significant instability, variability in temperatures and instabilities with observing mode should provide increased skepticism towards the analysis and any conclusion drawn from the inter-annual variability in the period of limb-staring.

Modeling:

We make use of the NASA ARC-MGCM version 2.1. *Nelli et al.* [2009] provides a description of this version of the model. The ARC-MGCM is a three-dimensional numerical global climate model adapted for Mars. The ARC-MGCM model solves the incompressible equations for fluid flow and heat transfer using finite difference techniques. The version we made use of applies an Arakawa C-grid [*Arakawa*, 1972]. The model was run with a 6°×5° latitude and longitude horizontal grid resolution. The model uses a normalized sigma-pressure coordinate system in the vertical direction. 30 vertical layers were employed, extending from the surface to 10^{-6} Pa. The model was run with a spatially & temporally uniform dust opacity, assuming a constant optical depth. All runs presented here were initialized from a "cold start" (i.e. uniform temperature and no initial wind), and run for 3 MYs before applying the effects of gravity waves.

H2010 suggested a link between enhanced gravity wave breaking at northern latitudes and low pressures (~0.1 Pa) and cooling at equatorial regions at 0.1 Pa before the MY28 global dust storm. Enhanced gravity wave breaking would result in enhanced damping of winds toward the phase velocity of the breaking waves. Because the ARC-MGCM is an incompressible model the effects of gravity waves are parameterized and applied as a drag to the winds. We specifically consider through our modeling the effect of an abrupt change in damping of the zonal

wind to a specified zonal phase speed at northern latitudes and low pressures (~0.1 Pa) to be consistent with the variability in convective instabilities observed by *H2010*. We explore zonal wind damping to the phase speed of 0 m/s and +/- 20 m/s. A phase speed of 0 m/s is typically representative of topographically forced gravity waves. However, the main source of gravity waves may not be topographic [*Creasey et al.*, 2006], so we have also explored damping to nonzero phase speeds. The damping was applied as a tendency and only when considering no other forces on a parcel, the scheme would result in an exponential decay in the zonal wind speed of a parcel to the prescribed phase speed. We have explored different e-folding times of 1×10^5s, 1×10^4s, and 1×10^3s when considering the exponential decay on the zonal wind speed of a parcel with no other forces acting on the parcel. The damping was applied equally at all longitudes. The damping is abruptly applied beginning at summer solstice (L_s 180°).. Instead of using the model temperature and wind fields to determine the location and magnitude of the damping, which is typical of gravity wave parameterization schemes (e.g. *Palmer et al.* [1986]), we have specified the time and magnitude of the damping, because we intended to explore the effect of abrupt changes in gravity wave breaking as observed by *H2010*.

Initial results indicate that zonal wind damping for all of our cases cannot reproduce the observed cooling at equatorial latitudes. Looking at modeled latitudinally averaged and time averaged temperatures between 1 Pa and 10 mPa near equatorial regions from 225° L_s, after zonal drag has been applied in the model, results in at most ~6 K cooling when compared against a run with no zonal wave drag applied. Important to note, cooling is not the largest with the strongest damping cases. Also, considering runs with damping only to 0 m/s, more consistent with topographically forced waves, cooling is at most ~4.5K when compared against a run with no drag applied. This is ~3 factors or more below what *H2010* observed. These results are in line with the cooling being the result of a limb staring mode calibration artifact.

Summary:

We have identified variability in limb staring temperatures and instabilities coincident with a change in MCS observing mode during MY28. We have conducted an analysis that suggests zero-signal offset variation can provide a non-negligible effect on whether instabilities are identified in derived MCS temperature profiles during limb staring. The analysis though is unable to conclude that variability in temperatures and instabilities are not present during MCS 'limb staring' operation. However, because the variability coincides with changes in observing modes, significant doubt about conclusions derived from the variability remains. We have also conducted modeling to explore whether the proposed gravity wave mechanism suggested by *H2010* can reproduce the observed cooling. The cooling magnitude we produce is a factor of 3-4 less than what *H2010* observed. This is in line with our current thinking that much of the observed cooling is the result of a limb staring observing mode artifact.

References:

Arakawa, A. (1972) Design of the UCLA general circulation model, *Department of Meteorology, University of California, Technical Report No. 7*, 64-76.

Creasey, J. E., J. M. Forbes, D. P. Hinson (2006), Global and seasonal distribution of gravity wave activity in Mars' lower atmosphere derived from MGS radio occultation data, *Geophys. Res. Lett., 33*, 1, L01803, doi: 10.1029/2005GL024037

Heave,ns N. G., M. I. Richardson, W. G. Lawson, C. Leea,b, D.J. McCleese, D.M. Kass, A. Kleinböhl, J.T. Schofield, W.A. Abdou & J.H. Shirley (2010), Convective instability in the martian middle atmosphere, *Icarus*, *208*, 574–589, doi: 10.1016/j.icarus.2010.03.023.

Kleinböhl, A., J. T. Schofield, D. M. Kass, W. A. Abdou, C. R. Backus, B. Sen, J. H. Shirley, W. G. Lawson, M. I. Richardson, F. W. Taylor, N. A. Teanby, & D. J. McCleese (2009), Mars Climate Sounder limb profile retrieval of atmospheric temperature, pressure, and dust and water ice opacity, *J. Geophys. Res.*, *114*, E10006, doi:10.1029/2009JE003358.

McCleese, D. J., J. T. Schofield, F. W. Taylor, S. B. Calcutt, M. C. Foote, D. M. Kass, C. B. Leovy, D. A. Paige, P. L. Read, & R. W. Zurek (2007), Mars Climate Sounder: An investigation of thermal and water vapor structure, dust and condensate distributions in the atmosphere, and energy balance of the polar regions, *J. Geophys. Res.*, *112*, E05S06, doi:10.1029/2006JE002790.

Nelli, S. M., J. R. Murphy, W. C. Feldman, & J. R. Schaeffer (2009), Characterization of the nighttime low-latitude water ice deposits in the NASA Ames Mars General Circulation Model 2.1 under present-day atmospheric conditions, *J. Geophys. Res.*, *114*, E11003, doi: 10.1029/2008JE003289

Palmer, T. N., G. J. Shutts & R. Swinbank (1986), Alleviation of a systematic westerly bias in general circulation and numerical weather prediction models through an orographic gravity wave drag parametrization, *Quart. J. R. Met. Soc.*, *112*, 1001-1039, doi: 10.1002/qj.49711247406.